

## Original Article

Adsorption kinetic of *Acinetobacter baylyi* for Cr (VI) removal under acidic conditionJittima Charoenpanich<sup>1, 2\*</sup>, Anongnart Khotthong<sup>1</sup>, Jutamas Pantab<sup>2</sup>,  
Noppamart Thasurin<sup>1</sup>, and Supattra Chumjam<sup>1</sup><sup>1</sup> Department of Biochemistry, Faculty of Science,  
Burapha University, Bangsaen, Mueang, Chon Buri, 20131 Thailand<sup>2</sup> Bioengineering Program, Faculty of Engineering,  
Burapha University, Bangsaen, Mueang, Chon Buri, 20131 Thailand

Received: 19 April 2021; Revised: 23 September 2021; Accepted: 24 November 2021

**Abstract**

Dried cell of a new strain, known as *Acinetobacter baylyi*, showed appropriate biological removal of Cr (VI) under acidic condition. The adsorption parameters optimised were: biomass dose (2.0 g/L), initial pH (2.0), agitation speed (250 rpm), initial Cr (VI) concentration (10–60 mg/L), temperature (30 °C), and time (72 h). The experimental data in the 20–60 mg/L Cr(VI) concentration range fitted well to the Langmuir isotherm ( $R^2 = 0.9545$ , maximum capacity 11.96 mg/g) and pseudo-second-order adsorption model. The adsorption mechanism was best described by the Boyd plot and an intraparticle diffusion model. TEM-EDX studies revealed that the noticeable chromium precipitates on bacterial surfaces and within the bacterial inner portions after Cr (VI) adsorption. An XPS study recommended that this bacterium use carbonyl/hydroxy/carboxy groups on the surface for adsorption of Cr (VI).

**Keywords:** biosorption, hexavalent chromium, *Acinetobacter baylyi*, kinetic model, isotherm study**1. Introduction**

An increasing growth in industrialisation and urbanisation has resulted in numerous serious consequences on the environment. Chromium (Cr) is one of the major contaminants in industrial effluents, which demands special treatment. The major sources of chromium release into the environment are water streams from electroplating, welding, alloy formation, leather tanning, electronic and metallurgy industries, among others (Mohan & Pittman, 2006). Chromium exists in several oxidation states between -2 and +6. Only the trivalent Cr(III) and hexavalent Cr(VI) stable oxidation forms have significant impacts on the environment (Richard & Bourg 1991). The United States Environmental Protection Agency stated Cr (VI) as one on the list of priority

pollutants (United States Environmental Protection Agency [USEPA], 2014). It is both carcinogenic and mutagenic to living organisms (IARC, 1987) and may cause damage to the kidney and lungs, in addition to its ability to cause skin ulcerations (Cieslak-Golonka, 1995). The USEPA announced that 0.1 mg/L is the allowable value for total chromium in drinking water (USEPA, 2017), while WHO proposed the discharge limit for Cr(VI) is <0.05 mg/L (World Health Organization [WHO], 2003). Thus, industries must manage chromium-contaminated wastewaters in a precise manner before discharging it to the environment. Several conventional technologies including chemical precipitation and ion-exchange separation are applied for the management of Cr (VI)-containing wastewater (Rengaraj, Yeon, & Moon, 2001). However, none of these methods can effectively and completely remove metals. Therefore, subsequent harmful secondary contamination remains, in spite of the high operating cost and demand of highly skilled labours.

\*Corresponding author

Email address: jittima@go.buu.ac.th

Adsorption of Cr (VI) using dried cell of appropriate microorganisms as bioadsorbent agents is an economical and promising strategy for treating of Cr(VI) contamination from aqueous effluents (Thatoi, Das, Mishra, Rath, & Das, 2014). However, the performance is limited by fluctuating conditions and the efficiency of Cr (VI) removal is species-dependent (Camargo, Bento, Okeke, & Frankenberger, 2003). Therefore, new bacteria that can overcome this limitation and be applied practically must be discovered. *Acinetobacter* are well represented among fermenting bacteria used as green degrader. Biotechnological contributions by *Acinetobacter* seem to imitate those of *Pseudomonas* sp. in terms of vigour and versatility. However, in contrast to *Pseudomonas*, the genome of *Acinetobacter* contains few traits involved for pathogenesis (Young, Parke, & Ornston, 2005). This study aimed to apply a dried cell of *Acinetobacter baylyi* (Uttatree, Winayanuwattikun, & Charoenpanich, 2010) for Cr (VI) removal. Experiments were also conducted to understand the mechanism of Cr (VI) adsorption and removal efficiency of the bacterium from a batch bioreactor system.

## 2. Materials and Methods

### 2.1 Dried cell preparation and morphological characterisation

This study used a marine bacterium, *Acinetobacter baylyi* (Uttatree *et al.*, 2010) as biosorbent. Cultivation and preparation of cell pellet were performed as described previously (Uttatree *et al.*, 2010). Dried cell of *A. baylyi* was prepared by dehydration of the cell pellet at 60°C for 3 days, followed by blending and sieving to retain particles between 0.1–0.5 mm before its usage. The cells with and without Cr (VI) were characterised by X-ray photoelectron spectroscopy (XPS) and transmission electron microscopy-energy dispersive X-ray (TEM-EDX) according to the methods of Cherdchoo, Nithetham, and Charoenpanich (2019).

### 2.2 Batch experiments

The Cr (VI) removal by dried cell of *A. baylyi* was continuously monitored in acrylic vessel (volume: 6 L, size 8" × 12") containing 5 L of synthetic wastewater (pH 2.0) amended with 10–60 mg/L Cr (VI) concentration for 96 h, at 30 °C and 250 rpm. The synthetic wastewater, which was used in this study, was prepared according to the works of Cherdchoo *et al.* (2019). One litre of synthetic wastewater contained 2.56 g of sodium acetate, 2.23 g of glucose, 43.9 mg of KH<sub>2</sub>PO<sub>4</sub>, 229.3 mg of NH<sub>4</sub>Cl, 90 mg of MgSO<sub>4</sub>·7H<sub>2</sub>O, 14 mg of CaCl<sub>2</sub>·2H<sub>2</sub>O and 0.3 mL of trace solution (1 L of trace solution contained 1.5 g of FeCl<sub>3</sub>·6H<sub>2</sub>O, 0.15 g of H<sub>3</sub>BO<sub>3</sub>, 0.03 g of CuSO<sub>4</sub>·5H<sub>2</sub>O, 0.18 g of KI, 0.12 g of MnCl<sub>2</sub>·H<sub>2</sub>O, 0.06 g of Na<sub>2</sub>MoO<sub>4</sub>·2H<sub>2</sub>O, 0.12 g of ZnSO<sub>4</sub>·7H<sub>2</sub>O, 0.15 g of CoCl<sub>2</sub>·6H<sub>2</sub>O and 10 g of ethylenediaminetetraacetic acid). The synthetic wastewater a pH ranging between 6.0–7.0, total chemical oxygen demand (COD) of 3,040 mg COD/L, soluble COD of 2,960 mg COD/L, mixed liquor suspended solid (MLSS) of 3.5 mg MLSS/L and ammonia nitrogen (NH<sub>4</sub><sup>+</sup>-N) of 34.70 mg N/L. The samples were withdrawn at regular time intervals and removed Cr(VI) was analysed, as describe below. Each set of experiments was performed triplicates and average ± SD values were reported.

### 2.3 Estimation of Cr (VI) concentration

Cr (VI) concentration at 540 nm wavelength was estimated by spectrophotometry after complexation with 1,5-diphenylcarbazide (APHA AWWA, 2005). A standard curve of Cr (VI) was conducted under 0–2 mg/L concentrations, generating an R<sup>2</sup> value of 0.9998. The amount of Cr (VI) in the supernatant was quantified. Synthetic wastewater without Cr (VI) was used as a control. Percentage of Cr (VI) removed was calculated using the following equation:

$$\text{Cr (VI) removal (\%)} = \frac{c_i - c_e}{c_i} \times 100 \quad (1)$$

Where “ $c_i$ ” and “ $c_e$ ” (mg/L) denote the concentration of Cr (VI) at the initial stage and after reduction, respectively. Each experiment was conducted in triplicate and the averages ± SD were reported.

Equilibrium adsorption capacity  $q_e$  (mg/g) and adsorption capacity at different time “ $t$ ”,  $q_t$  (mg/g) were calculated, respectively, as follows:

$$q_e = \frac{(c_i - c_e)}{m} V \quad (2)$$

$$q_t = \frac{(c_i - c_t)}{m} V \quad (3)$$

Where “ $c_i$ ”, “ $c_e$ ” and “ $c_t$ ” indicate Cr (VI) concentration (mg/L) at initial, equilibrium and time “ $t$ ” (min), respectively;  $m$  is the mass of dried cell bacteria (g) and  $V$  is the volume of Cr (VI) solution (L).

### 2.4 Isotherm studies

The equilibrium isotherms were measured against 20–60 mg/L Cr(VI) concentrations in 50 mL of synthetic wastewater (pH 2.0). Experiments were performed at 30°C, 250 rpm and 2 g/L biomass dose for 96 h to ensure the attainment of adsorption equilibrium. The average values from three times experiments were used for analysis. The Langmuir and Freundlich isotherm models were examined with the experimentally “ $q_e$ ” value obtained from equilibrium (Freundlich, 1906; Langmuir, 1916).

### 2.5 Langmuir isotherm

Langmuir model quantitatively describes the maximum adsorption on saturated monolayer of adsorbent surface (Langmuir, 1916). The experimental data were fitted to the Langmuir equation:

$$\frac{c_e}{q_e} = \frac{1}{q_m} c_e + \frac{1}{K_L q_m} \quad (4)$$

Where “ $c_e$ ” (mg/L) is the equilibrium concentration of Cr(VI) in solution, “ $q_e$ ” (mg/g) is the amount of Cr(VI) adsorbed at equilibrium, and “ $q_m$ ” and “ $K_L$ ” are the monolayer adsorption capacity (mg/g) and Langmuir equilibrium constant (L/mg) which indicates the nature of adsorption, respectively.

Langmuir adsorption parameters were determined by rearranges the Langmuir equation (Equation 4) into linear form as follow:

$$\frac{1}{q_e} = \left( \frac{1}{q_m K_L} \right) \left( \frac{1}{c_e} \right) + \frac{1}{q_m} \quad (5)$$

The values of “ $q_m$ ” and “ $K_L$ ” were determined by the plot of  $1/q_e$  versus  $1/c_e$  producing a straight line of slope  $1/q_m K_L$  and the intercept  $1/q_m$  that corresponded to complete monolayer coverage.

Further analysis of Langmuir isotherm could be used to explain affinity between the adsorbent and Cr(VI) in terms of dimensionless constant called equilibrium parameter ( $R_L$ ) defined by the following relationship:

$$R_L = \frac{1}{1 + K_L c_e} \quad (6)$$

Where “ $K_L$ ” is the Langmuir constant and “ $c_e$ ” is the equilibrium concentration of Cr(VI) in solution (mg/L). The value of  $R_L$  indicates information as to whether adsorption may be described as:  $R_L > 1$  unfavorable,  $R_L = 1$  linear,  $0 < R_L < 1$  favorable, and  $R_L = 0$  irreversible.

## 2.6 Freundlich isotherm

Freundlich model is the isotherm used to describe adsorption characteristic of heterogeneous or multilayer surface (Freundlich, 1906). The Freundlich adsorption equation takes the following general form:

$$q_e = K_f c_e^{1/n} \quad (7)$$

Where “ $q_e$ ” and “ $c_e$ ” have the same meaning as in Langmuir isotherm and “ $K_f$ ” and “ $n$ ” are the Freundlich constants representing the indicator of adsorption capacity and intensity, respectively.

Freundlich equation can be described by the linear form as:

$$\log q_e = \log K_f + \frac{1}{n} \log c_e \quad (8)$$

The linear plot of  $\log q_e$  versus  $\log c_e$  gives straight line of slope  $1/n$  and the intercept is  $\log K_f$ . The value of  $1/n$  indicates type of isotherms as:  $1/n < 1$  normal adsorption and  $1/n > 1$  cooperative adsorption.

## 2.7 Kinetic studies

The adsorption kinetic experiments were conducted at 30°C and pH 2.0. Kinetic curves were acquired at a predetermined time interval of 12 h for 96 h. The pseudo-first-order and pseudo-second-order adsorption (Qiu *et al.*, 2009), intraparticle diffusion (Hameed & Ahmad, 2009) and Boyd models (Boyd, Adamson, & Myers, 1947) were fitted to the experimental data. Two classical reduction models, pseudo-

first-order and pseudo-second-order were also examined (Park, Lim, Yun, & Park, 2007).

## 2.8 Pseudo-first-order model (Lagergren model)

Lagergren proposed a first-order rate of equation for analysis of liquid-solid phase adsorption (Qiu *et al.*, 2009). It can be expressed as follows:

$$\frac{dq_t}{dt} = k_1 (q_e - q_t) \quad (9)$$

Integrating Equation (9), for the boundary conditions  $t = 0$  to  $t = t$  and  $q_t = 0$  to  $q_t = q_t$  gives

$$\frac{\ln(q_e - q_t)}{q_e} = -k_1 t \quad (10)$$

The non-linear form of pseudo-first-order model kinetic equations as:

$$q_t = q_e (1 - e^{-k_1 t}) \quad (11)$$

The linear form of pseudo-first-order model is generally expressed as follows:

$$\log(q_e - q_t) = \log q_e - \frac{k_1}{2.303} t \quad (12)$$

Where “ $q_t$ ” (mg/g) is the adsorption capacity at time “ $t$ ” (min), “ $q_e$ ” (mg/g) is the equilibrium capacity, and “ $k_1$ ” is the pseudo-first-order rate constant.

The plots of  $\log(q_e - q_t)$  versus  $t$  shows the slope and intercept as  $k_1$  (pseudo-first-order rate constant) and  $q_e$  (equilibrium capacity), respectively.

## 2.9 Pseudo-second-order model

The adsorption kinetic may also be described by the pseudo-second-order model that was purposed by Ho and Mckay (Qiu *et al.*, 2009). The rate of reaction is represented as follows:

$$\frac{dq_t}{dt} = k_2 (q_e - q_t) \quad (13)$$

Integrating Equation (13), for boundary condition  $t = 0$  to  $t = t$  and  $q_t = 0$  to  $q_t = q_t$  gives

$$q_t = \frac{k_2 q_e^2 t}{1 + k_2 q_e t} \quad (14)$$

This is integrated rat law for a pseudo-second-order model chemisorptions reaction (Equation 14) which can be rearranged as:

$$\frac{t}{q_t} = \frac{1}{k_2 q_e^2} + \frac{1}{q_e} t \quad (15)$$

Where “ $q_t$ ” (mg/g) is the adsorption capacity at time “ $t$ ” (min), “ $q_e$ ” (mg/g) is the equilibrium capacity, and “ $k_2$ ” is the pseudo-second-order rate constant.

The plot of  $1/q_t$  versus  $t$  at different Cr(VI) concentrations gives a straight line with slope of  $1/k_2q_e^2$  and intercept of  $1/q_e$ .

### 2.10 Intra-particle diffusion model (Morris-Weber equation)

The intra-particle diffusion is the rate controlling step recommended for investigation (Hameed and Ahmad, 2009). This kinetic model was proposed by Weber and Morris as follows:

$$q_t = k_{id}t^{0.5} + \theta \quad (16)$$

Where “ $q_t$ ” (mg/g) is the amount of Cr(VI) on the adsorbent surface at time “ $t$ ” (min<sup>0.5</sup>) and “ $k_{id}$ ” is the intra-particle diffusion rate constant (mg/g min<sup>0.5</sup>) and  $\theta$  is a parameter which its value is depending on film diffusion (external diffusion) in the kinetics adsorption.

The plot of  $q_t$  versus  $t^{0.5}$  gives a straight line. The adsorption process controlled by intra-particle diffusion shows the intercept is  $\theta$  indicating the boundary thickness layer.

### 2.11 Boyd plot

Boyd plot is typically used to confirm the role of external mass transfer during the adsorption process (Boyd *et al.*, 1947). The model is represented as follows:

$$B_t = -0.4977 - \ln(1 - F) \quad (17)$$

Where “ $F$ ” is the fraction of solute adsorbed at time “ $t$ ” (min) is given by “ $q_t/q_e$ ”, and “ $B_t$ ” is the calculated value obtained from the equation.

### 2.12 Reduction model

Kinetic models based on reduction were also applied to fit the experimental data of Cr(VI) adsorption by the bacterium. These used to confirm whether adsorption mechanism occurred by “anionic adsorption” or “adsorption-coupled reduction” (Park *et al.*, 2007).

Pseudo-first-order reduction:

$$\ln C = \ln C_0 - k_3t \quad (18)$$

Pseudo-second-order reduction:

$$\frac{1}{C} = k_4t + \frac{1}{C_0} \quad (19)$$

Where “ $C_0$ ” and “ $C$ ” are Cr(VI) concentrations in solution (mg/L) at time “ $0$ ” and “ $t$ ” respectively, and “ $k_3$ ” and “ $k_4$ ” are the apparent rate constants (min<sup>-1</sup>).

### 2.13 Best fitting model estimation

The experimental data that best fit the kinetic

models was estimated based on the  $R^2$  values obtained from a linear plot of the equation model and Marquardt’s present SD (MPSD) developed by Marquardt (Marquardt 1963). MPSD was calculated using the following equation:

$$MPSD = 100 \left( \sqrt{\frac{1}{p-n} \sum_{i=1}^p \left[ \frac{q_{t,exp} - q_{t,calc}}{q_{t,exp}} \right]^2} \right) \quad (20)$$

Where “ $p$ ” is the number of experimental data points and “ $n$ ” is the number of parameters in the model equation. “ $q_{t,exp}$ ” and “ $q_{t,calc}$ ” refer to the experimental and calculated values from the model equation, respectively. A small MPSD reveals the accurate estimation of  $q_t$ .

## 3. Results and Discussion

### 3.1 Monitoring of Cr (VI) removal

Living and dried cell of *Acinetobacter baylyi* (Uttaree *et al.* 2010) was initially tested for the removal of 20 mg/L initial Cr (VI) concentration in synthetic wastewater (pH 7.0) at 30°C and 250 rpm. The % Cr (VI) removal and adsorption capacity had a similar pattern, which strongly depends on the incubation time. The removal efficiency increased continuously and attained equilibrium after 48 h and 15 h of incubation for living and dried cell, respectively. Since the dried cell of *A. baylyi* could completely remove Cr (VI) faster than the living cell and gave higher adsorption capacity (3.5 mg/g for dried cell and 2.0 mg/g for living cell), the dried cell was recommended for use as an adsorbent agent for Cr (VI) removal in all studies.

A time-course study for Cr (VI) adsorption by *A. baylyi* dried cell was performed (Figure 1). Cr (VI) was rapidly removed in the initial stages of cultivation, then an efficiency was slower and attained equilibrium at 72 h. A rich of Cr (VI) ion during the early stage of the adsorption might drive ion diffusion and uptake to the bacterial cell. The slower adsorption rate before equilibrium was result of the limited surface area adsorbed and the small concentration of Cr (VI) ion. Hence, throughout the results, the cultivation time of 72 h was selected as the equilibration time for the isotherm studies.

### 3.2 Characterization of the bacterial cell after Cr (VI) adsorption

The TEM images showed the accumulation of chromium particles on the surface and inside of the bacterial cells after Cr (VI) adsorption (Figure 2). The EDX study revealed the contribution of C and O ions as common elements on the bacterial cell and some chromium peaks with 0.08 wt% were detected for Cr (VI)-treated cells. These results are consistent with those of previous studies reporting the accumulation of chromium within bacterial cells (Das *et al.* 2014).

The XPS survey spectra indicate that dried cell of *A. baylyi* consisted carbon (B.E. = 284.9 eV, C1s) and oxygen (B.E. = 531.9 eV, O1s). A drop of % atomic concentration of carbon and oxygen from 63.39% to 50.86% and from 21.25% to 17.48%, respectively was found after Cr (VI) adsorption. This suggests a possible contribution of the carbon and

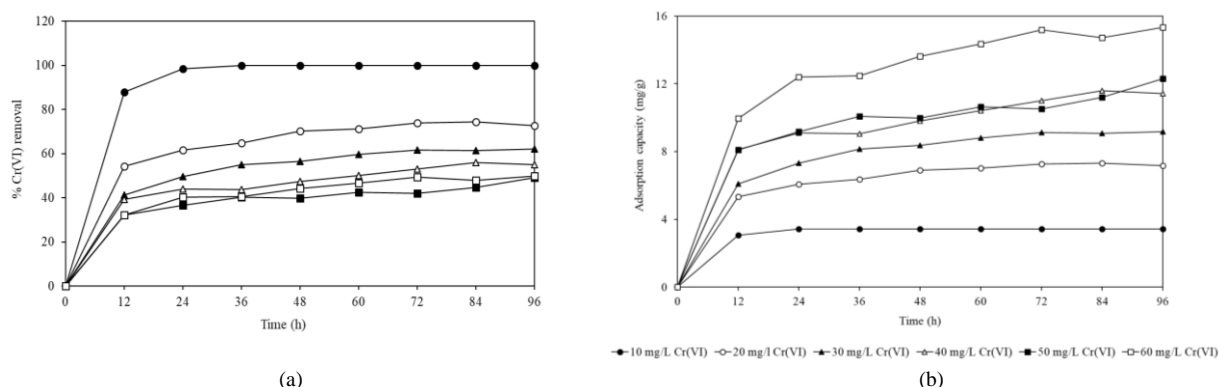


Figure 1. Time-course study of Cr (VI) removal by dried cell of *A. baylyi* at different initial Cr (VI) concentrations. Experimental conditions: 30°C, 2 g/L biomass dose, pH 2.0 and 250 rpm

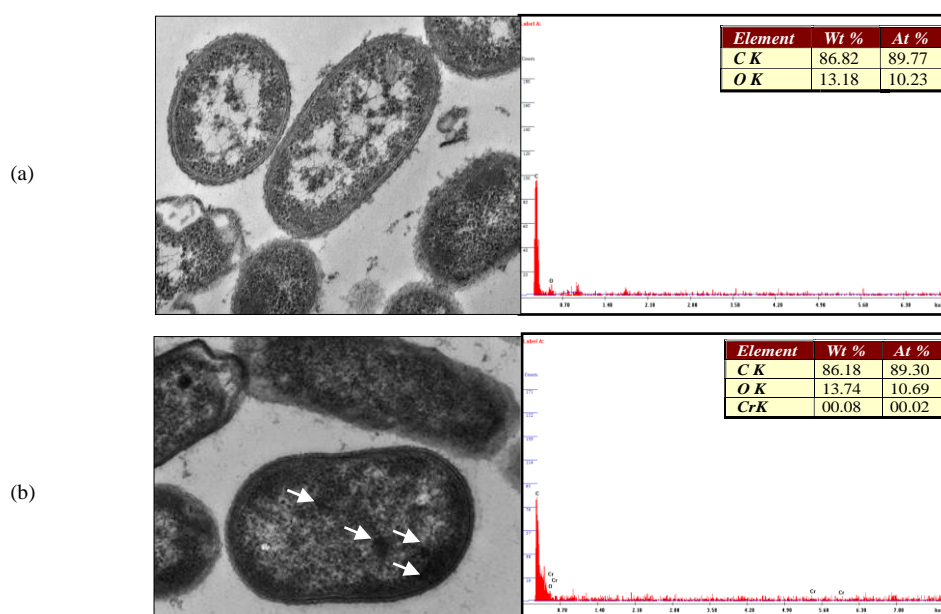


Figure 2. TEM images and EDS analysis of *A. baylyi* (a) before and (b) after cultivation in synthetic wastewater (pH 7.0) containing 20 mg/L Cr (VI) at 30°C and 250 rpm for 24 h. White arrows represent the chromium accumulation within the bacterial cell.

oxygen functional groups in Cr (VI) adsorption (Li, Cao, & Zhang, 2008). A comparison of the XPS spectra correlating to the C1s and O1s of the bacterial cell surface with and without Cr(VI) was performed. The XPS C1s spectrum of *A. baylyi* after contact with Cr (VI) (Figure 3a) shows that the shift of component peaks correspond to the hydroxy group (C-O, B.E. = 286.37 eV, 22.9%), carbonyl groups (C=O, B.E. = 288.10 eV, 10.8%) and carboxy group (O-C=O, B.E. = 289.14 eV, 2.9%). In the same way, the XPS O1s spectrum (Figure 3b) shows the involvement of hydroxy/carbonyl/ carboxy groups during the Cr (VI) adsorption. The changes in the peaks highlighted that the carbonyl/hydroxy/carboxy groups on the surface and inside of *A. baylyi* are associated with Cr (VI) adsorption.

### 3.3 Equilibrium isotherms and kinetic studies

The mechanism of Cr (VI) adsorption by *A. baylyi* was elucidated using Langmuir and Freundlich models. Table

1 shows the experimental data evaluated by the equilibrium isotherm models. The linear portion of adsorption isotherm are presented in Figure 4. The Langmuir model ( $R^2 = 0.9545$ ) describes the adsorption of Cr (VI) by *A. baylyi* better than the Freundlich model ( $R^2 = 0.7964$ ). This result recommends a monolayer adsorption of Cr (VI) on heterogeneous surfaces. The maximum adsorption capacity ( $q_m$ ) and Langmuir equilibrium constant ( $K_L$ ) were estimated as 11.96 mg/g and 0.301 L/mg, respectively. The calculated equilibrium parameter ( $R_L$ ) for the adsorption of Cr (VI) on the bacterial cells were between 0.051–0.145, representing the favourable adsorption of Cr (VI) with bacterial cells under the study conditions.

Two classical adsorption kinetic models were applied to the experimental data for better understanding of the possible mechanism underlying the removal of Cr (VI) by *A. baylyi* dried cell. Table 2 and Figure 5 reveal that the pseudo-second-order model matches well with the experimental data (since  $R^2$  close to unity) when compared to

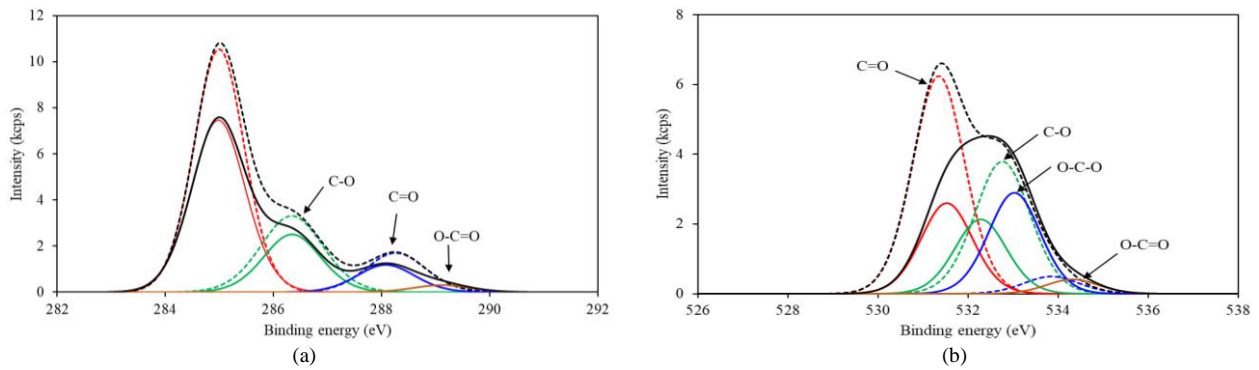


Figure 3. Comparison of XPS spectra of *A. baylyi* before (dotted lines) and after (linear) treatment with Cr (VI). High-resolution spectra of (a) C1s and (b) O1s

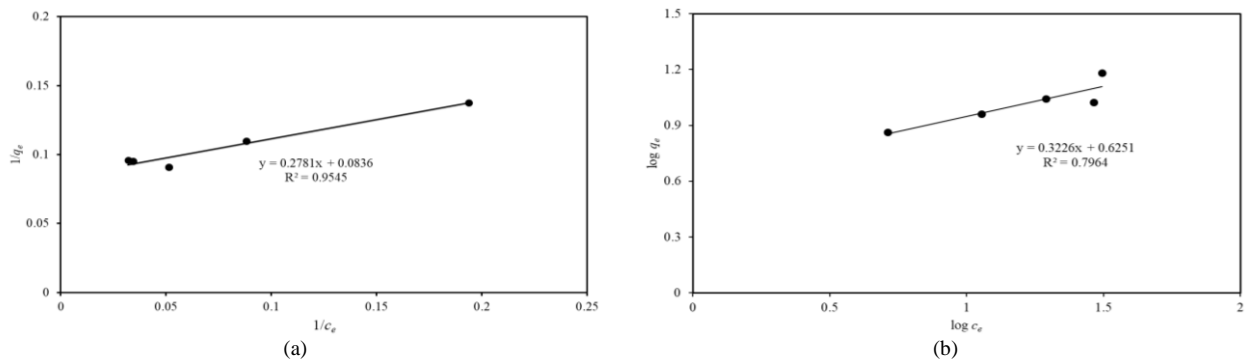


Figure 4. (a) Langmuir isotherm and (b) Freundlich isotherm for Cr (VI) adsorption by *A. baylyi* at 20–60 mg/L Cr (VI) concentrations. Experimental conditions: 30°C, 2 g/L biomass dose, pH = 2.0 and 250 rpm

Table 1. Isotherm parameters for Cr (VI) adsorption by dried cells of *A. baylyi*

Langmuir parameters				Freundlich parameters			
K <sub>L</sub> (calculated) (L/mg)	R <sub>L</sub> (L/mg)	q <sub>m</sub> (mg/g)	R <sup>2</sup>	K <sub>f</sub> (calculated) (mg/g)	1/n	n	R <sup>2</sup>
0.301	0.051–0.145 0 < R <sub>L</sub> < 1	11.96	0.9545	4.218	0.323	3.100	0.7964

the pseudo-first-order model. This was confirmed by MPSD values < 12. Thus, given the comparison of the R<sup>2</sup> and MPSD values, the pseudo-second-order equation was considered appropriate for modelling the Cr (VI) adsorption.

The linear plot of an intraparticle diffusion model (Figure 5c) did not pass through the origin. This indicates that pore diffusion was not the sole rate-controlling step. Boyd plot was also used to further confirm the role of external mass transfer during the adsorption process of Cr (VI) by *A. baylyi*. If the linear plot passes through the origin, then the adsorption is driven by particle diffusion; otherwise, it is controlled by film diffusion (Rorrer & Hsien, 1993). From Figure 6, the plot was linear, but did not pass through the origin, thus indicating that film diffusion controlled the adsorption process at the investigated concentrations.

After fitting the experimental data to the reduction kinetic models (Figure 7), the results showed that the Cr(VI) removal by *A. baylyi* was inconsistent with both kinetic equations. The R<sup>2</sup> values obtained from the linear plots of both equations (Table 3) were relatively small. The concentration (c<sub>e</sub>) calculated by the model deviated from those determined by the experiments, which were confirmed by

high MPSD values, making both equations inconsistent for the removal of Cr (VI) by the bacterium.

From the results, the mechanism underlying Cr (VI) removal by *A. baylyi* may consist of the following four steps: (1) migration of Cr(VI) ions from the solution to the bacterial cell surface; (2) monolayer and chemisorption in the film covering the bacterial cell surface; (3) transport of chromium ions from the bacterial cell surface to the interior pores of the cell particles; and (4) intracellular bioaccumulation of chromium and its reduction to other forms.

Although there are documents describing the potential of *Acinetobacter* sp. for Cr (VI) removal, there is no report on the adsorption mechanism (Bhattacharya *et al.* 2014; Mrudula *et al.* 2012; Narayani & Shetty K 2012; Ontañon, González, & Agostini, 2015; Pei, Shahir, Raj, Zakaria, & Ahmad, 2009). Thus, this report completes the kinetic mechanism of Cr (VI) adsorption by *Acinetobacter* genera. A quick removal of Cr (VI) and an efficiency under acidic condition makes this bacterium an attractive agent for the biotreatment of Cr (VI) generated from industries, especially the tannery wastewater (Islam, Musa, Ibrahim, Sharafa, & Elfaki, 2014).

Table 2. Kinetic constants for Cr (VI) adsorption by dried cells of *A. baylyi*

Experimental	Kinetic model constants, R <sup>2</sup> and MPSD														
	Pseudo-first-order adsorption					Pseudo-second-order adsorption				Intraparticle diffusion			Boyd plot		
Cr(VI) (mg/L)	q <sub>e,exp</sub> (mg/g)	q <sub>e,calc</sub> (mg/g)	k <sub>1</sub> (min <sup>-1</sup> )	R <sup>2</sup>	MPSD	q <sub>e,calc</sub> (mg/g)	k <sub>2</sub> (min <sup>-1</sup> )	R <sup>2</sup>	MPSD	q <sub>e,calc</sub> (mg/g)	k <sub>id</sub> (min <sup>-1</sup> )	Θ	R <sup>2</sup>	MPSD	R <sup>2</sup>
20	7.263	5.037	0.053	0.9557	86.17	7.134	0.021	0.9985	3.24	7.372	0.393	4.0374	0.9506	3.46	0.9718
30	9.116	6.911	0.052	0.9704	61.60	8.969	0.012	0.9994	2.09	8.939	0.475	4.9081	0.9190	5.26	0.9763
40	11.015	6.782	0.041	0.8867	133.49	11.004	0.008	0.9910	11.59	10.876	0.564	6.0940	0.9591	3.38	0.8975
50	10.527	6.958	0.064	0.8882	98.25	11.167	0.008	0.9845	9.88	11.047	0.558	6.3093	0.9243	4.29	0.8282
60	15.198	10.592	0.043	0.9378	87.01	14.734	0.006	0.9963	5.21	14.656	0.808	7.8003	0.9281	5.15	0.9465

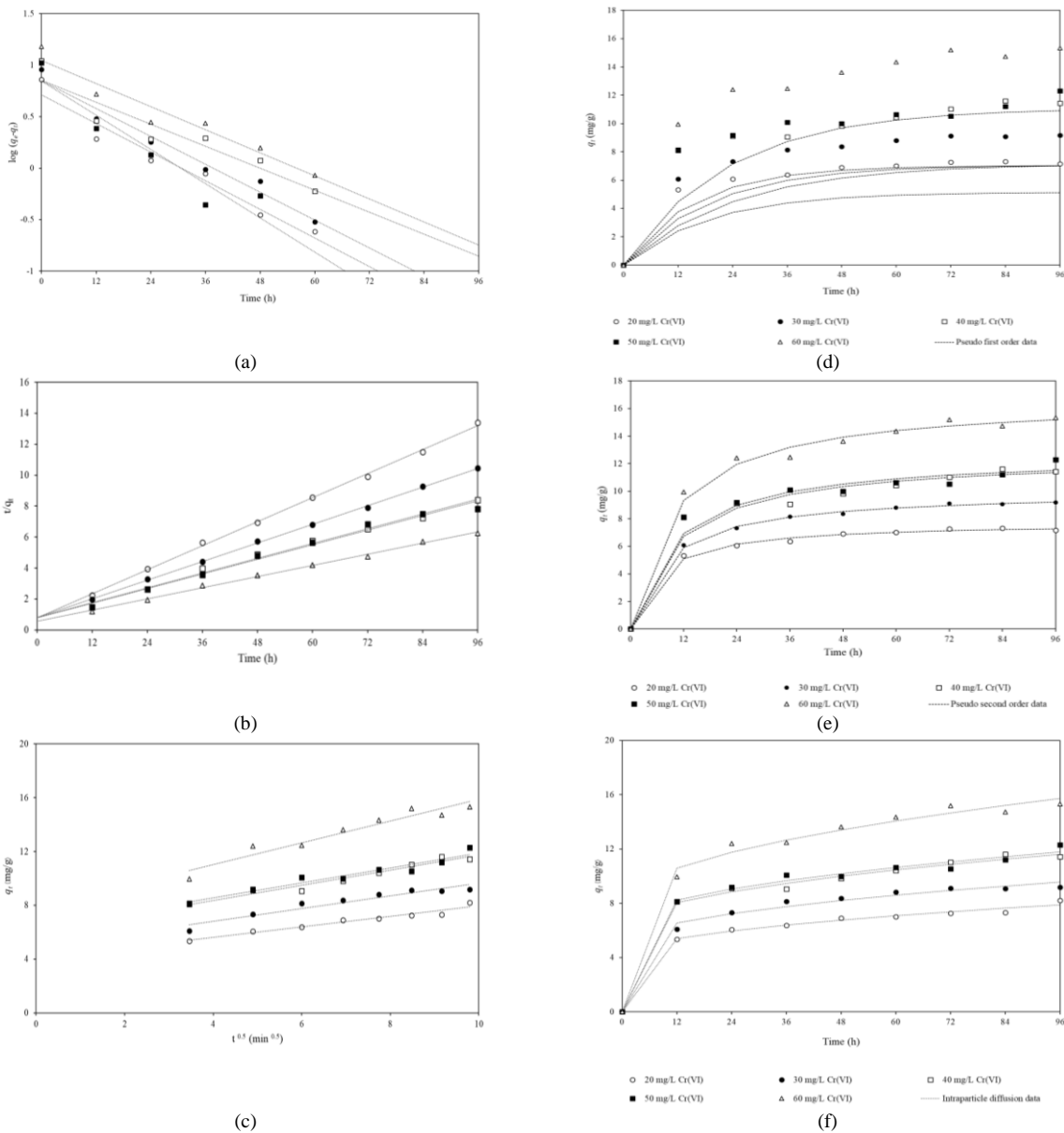


Figure 5. Linear and non-linear plots for the adsorption kinetic studies of Cr (VI) by *A. baylyi* at 20–60 mg/L Cr (VI) concentrations. (a, d) Pseudo-first-order model; (b, e) pseudo-second-order model; (c, f) intraparticle diffusion model. Symbols represent the experimental data and dotted lines imply theoretical data fitting of the model. Experimental conditions: pH 2.0, 250 rpm agitation speed, 30°C and 2 g/L bacterial biomass

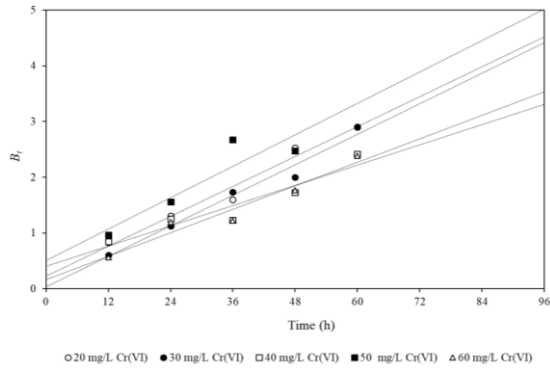


Figure 6. Boyd plot for Cr (VI) removal by *A. baylyi*. Experimental conditions were pH 2.0, 250 rpm agitation speed, 30°C and 2 g/L bacterial biomass

#### 4. Conclusions

This study evaluates the application of *A. baylyi* dried cell for Cr(VI) adsorption under acidic condition. TEM-EDX image revealed the chromium accumulation on the surface and inside of the cell after Cr (VI) adsorption. XPS analysis suggested the bacterium uses carbonyl/hydroxy/carboxy groups for Cr(VI) adsorption. Isotherm and kinetic studies indicated a monolayer and chemisorption in the film covering the bacterial surface. Thereafter, the Cr (VI) ions were transported and accumulated in the bacterial cell through pore diffusion. The results obtained from this study offers a potential advantage for the application of *A. baylyi* dried cell in bioremediation of Cr (VI) contamination.

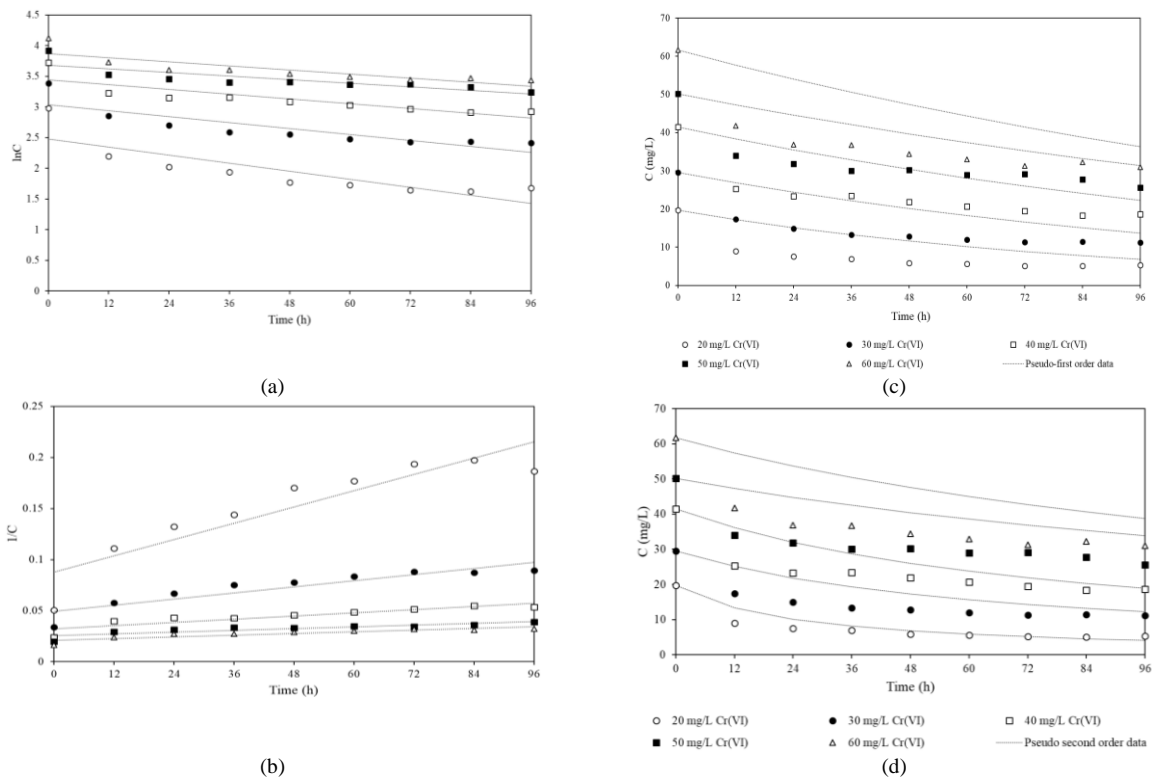


Figure 7. Linear and non-linear plots for the reduction kinetic studies of Cr (VI) by *A. baylyi* at 20–60 mg/L Cr (VI) concentrations. (a, c) Pseudo-first-order plot and (b, d) pseudo-second-order plot. Experimental conditions: pH 2.0, 250 rpm agitation speed, 30°C and 2 g/L bacterial biomass

Table 3. Kinetic constants for Cr (VI) reduction by dried cells of *A. baylyi*

Experimental	Kinetic model constants, R <sup>2</sup> and MPSD								
	Pseudo-first-order reduction					Pseudo-second-order reduction			
	Cr(VI) (mg/L)	C <sub>e,exp</sub> (mg/L)	C <sub>e,calc</sub> (mg/L)	k <sub>3</sub> (min <sup>-1</sup> )	R <sup>2</sup>	MPSD	C <sub>e,calc</sub> (mg/L)	k <sub>4</sub> (min <sup>-1</sup> )	R <sup>2</sup>
20	5.165	8.919	0.011	0.7008	113.63	5.134	0.002	0.8344	34.25
30	11.345	16.626	0.008	0.7179	72.83	14.325	0.001	0.8234	48.29
40	19.489	26.002	0.007	0.7269	55.60	21.889	0	0.8273	33.84
50	29.136	35.269	0.005	0.6875	44.57	36.867	0	0.7655	49.18
60	31.263	41.497	0.006	0.7035	48.62	42.702	0	0.7828	50.83

## Acknowledgements

This research was supported by a Research Grant of Burapha University (Grant no. 204/2561) awarded to J.C. We would like to thank the graduate research assistant (GRA) scholarship awarded to J.P from Faculty of Engineering, Burapha University. We also thank Faculty of Science, Burapha University for the partial granted of senior project.

## References

- American Public Health Association, American Water Works Association. (2005). *Standard methods for the examination of water and wastewater* (25<sup>th</sup> ed.). Washington, DC: Centennial.
- Boyd, G. E., Adamson, A. W., & Myers, Jr. L. S. (1947). The exchange adsorption of ions from aqueous solutions by organic zeolites, II: kinetics. *Journal of The American Chemical Society*, 69, 2836-2848.
- Camargo, F. A. O., Bento, F. M., Okeke, B. C., & Frankenberger, W. T. (2003). Chromate reduction by chromium-resistant bacteria isolated from soils contaminated with dichromate. *Journal of Environmental Quality*, 32, 1228-1233.
- Cherdchoo, W., Nithettham, S., & Charoenpanich, J. (2019). Removal of Cr(VI) from synthetic wastewater by adsorption onto coffee ground and mixed waste tea. *Chemosphere*, 221, 758-767.
- Cieslak-Golonka, M. (1995). Toxic and mutagenic effects of chromium (VI): A review. *Polyhedron*, 15, 3667-3689.
- Das, S., Mishra, J., Das, S. K., Pandey, S., Rao, D. S., Chakraborty, A., . . . Thatoi, H. (2014). Investigation on mechanism of Cr(VI) reduction and removal by *Bacillus amyloliquefaciens*, a novel chromate tolerant bacterium isolated from chromite mine soil. *Chemosphere*, 96, 112-121.
- Freundlich, H. M. F. (1906). Over the adsorption in solution. *Journal of Physical Chemistry*, 57, 385-471.
- Hameed, B. H., & Ahmad, A. A. (2009). Batch adsorption of methylene blue from aqueous solution by garlic peel, an agricultural waste biomass. *Journal of Hazardous Materials*, 164, 870-875.
- IARC. (1987). Monographs on the evaluation of carcinogenic risks to humans: Overall evaluation of carcinogenicity. An updating of IARC Monographs, France.
- Islam, B. I., Musa, A. E., Ibrahim, E. H., Sharafa, S. A. A., & Elfaki, B. M. (2014). Evaluation and characterization of tannery wastewater. *Journal of Forest Products and Industries*, 3, 141-150.
- Langmuir, I. (1916). The evaporation, condensation and reflection of molecules and the mechanism of adsorption. *Physical Review*, 8(2), 149-176.
- Li, X., Cao, J., & Zhang, W. (2008). Stoichiometry of Cr(VI) immobilization using nanoscale zerovalent iron (nZVI): a study with high-resolution X-ray photo electron spectroscopy (HR-XPS). *Industrial and Engineering Chemistry Research*, 47, 2131-2139.
- Marquardt, D. W. (1963). An algorithm for least-squares estimation of nonlinear parameters. *SIAM Journal on Applied Mathematics*, 11, 431-441.
- Mohan, D., & Pittman, C. U. (2006). Activated carbons and low cost adsorbents for remediation of tri- and hexavalent chromium from water. *Journal of Hazardous Materials*, 137, 762-811.
- Narayani, M., & Shetty, K. V. (2012). Characteristics of a novel *Acinetobacter* sp. and its kinetics in hexavalent chromium bioreduction. *Journal of Microbiology and Biotechnology*, 22(5), 690-698.
- Ontañón, O. M., González, P. S., & Agostini, E. (2015). Biochemical and molecular mechanisms involved in simultaneous phenol and Cr(VI) removal by *Acinetobacter guillouiae* SFC 500-1A. *Environmental Science and Pollution Research*, 22, 13014-13023.
- Park, D., Lim, S. R., Yun, Y. S., & Park, J. M. (2007). Reliable evidences that the removal mechanism of hexavalent chromium by natural biomaterials is adsorption-coupled reduction. *Chemosphere*, 70 (2), 298-305.
- Pei, Q. H., Shahir, S., Raj, A. S. S., Zakaria, Z. A., & Ahmad, W. A. (2009). Chromium (VI) resistance and removal by *Acinetobacter haemolyticus*. *World Journal of Microbiology and Biotechnology*, 25, 1085-1093.
- Qiu, H., Lv, L., Pan, B. - C., Zhang, Q. - J., Zhang, W. - M., & Zhang, Q. - X. (2009). Critical review in adsorption kinetic models. *Journal of Zhejiang University-SCIENCE A*, 10, 716-724.
- Rengaraj, S., Yeon, K. - H., & Moon, S. - H. (2001). Removal of chromium from water and wastewater by ion exchange resins. *Journal of Hazardous Materials*, 87, 273-287.
- Richard, F. C., & Bourg, A. C. M. (1991). Aqueous geochemistry of chromium: A review. *Water Research*, 25, 807-816.
- Rorrer, G. L., & Hsien, T. (1993). Synthesis of porous-magnetic chitosan beads for removal of cadmium ions from wastewater. *Industrial and Engineering Chemistry Research*, 32, 2170-2178.
- Thatoi, H., Das, S., Mishra, J., Rath, B. P., & Das, N. (2014). Bacterial chromate reductase, a potential enzyme for bioremediation of hexavalent chromium: a review. *Journal of Environmental Management*, 146, 383-399.
- United States Environmental Protection Agency. (2014). Retrieved from <https://www.epa.gov/sites/production/files/2015-09/documents/priority-pollutant-list-epa.pdf>.
- United States Environmental Protection Agency. (2017). Retrieved from <https://www.epa.gov/sdwa/chromium-drinking-water>.
- Uttatree, S., Winayanuwattikun, P., & Charoenpanich, J. (2010). Isolation and characterization of a novel thermophilic-organic solvent stable lipase from *Acinetobacter baylyi*. *Applied Biochemistry and Biotechnology*, 162, 1362-1376.

- World Health Organization. (2003). Retrieved from [https://www.who.int/water\\_sanitation\\_health/dwq/chemicals/chromium.pdf](https://www.who.int/water_sanitation_health/dwq/chemicals/chromium.pdf).
- Young, D. M., Parke, D., & Ornston, L. N. (2005). Opportunities for genetic investigation afforded by *Acinetobacter baylyi*, a nutritionally versatile bacterial species that is highly competent for natural transformation. *Annual Review of Microbiology*, 59, 519-551.